Toll-like receptor 4 modulates cell migration and cortical neurogenesis after focal cerebral ischemia

Ana Moraga,[1] Jesús M. Pradillo,[1] María I. Cuartero, Macarena Hernández-Jiménez, Marta Oses, María A. Moro, and Ignacio Lizasoain[2]

Unidad de Investigación Neurovascular, Departamento de Farmacología, Facultad de Medicina, Universidad Complutense, Madrid, Spain

ABSTRACT **Toll-like receptor 4 (TLR4) mediates brain damage after stroke. Now our objective is to determine TLR4 involvement in stroke-induced neurogenesis. Stroke was induced by permanent middle cerebral artery occlusion in wild-type and TLR4-deficient mice. Stereological and densitometric analysis of immunofluorescence-labeled brain sections and FACS analysis of cell suspensions were performed. Our results show that subventricular zone (SVZ) cell proliferation after stroke depends on infarct size. Second, when comparing brains with similar lesions, TLR4 attenuated SVZ proliferation, as shown by a decrease in prominin-1$^+$/EGFR$^+$/nestin$^-$ cells (type-C cells) at 1–2 d, and in BrdU$^+$ cells at 7 d, in *TLR4*$^{+/+}$ *vs. TLR4*$^{-/-}$ mice. Interestingly, 7 d after the infarct, neuroblasts in *TLR4*$^{+/+}$ mice migrated farther distances, reaching areas closer to the lesion than those in TLR4-deficient mice. However, at 14 d, TLR4-deficient mice presented a higher number of neuroblasts in all migratory zones than the *TLR4*$^{+/+}$ counterparts, which suggests that TLR4 deficiency delays neuroblast migration. Consistently, *TLR4*$^{+/+}$ mice showed an increased number of interneurons (NeuN$^+$/BrdU$^+$/GAD67$^+$ cells) in peri-infarct cortex 14–28 d after stroke. Our data indicate that, despite a negative effect on SVZ cell proliferation, TLR4 plays an important role in stroke-induced neurogenesis by promoting neuroblasts migration and increasing the number of new cortical neurons after stroke.—Moraga, A., Pradillo, J. M., Cuartero, M. I., Hernández-Jiménez, M., Oses, M., Moro, M. A., Lizasoain, I. Toll-like receptor 4 modulates cell migration and cortical neurogenesis after focal cerebral ischemia. *FASEB J.* 28, 4710–4718 (2014). www.fasebj.org**

Key Words: innate immunity · neuroblast · proliferation · stroke

Abbreviations: APC, anti-prominin1/CD133; BrdU, 5-bromo-2′-deoxyuridine; DCX, doublecortin; EGFR, epidermal growth factor receptor; GAD67, glutamic acid decarboxylase 67; MCA, middle cerebral artery; MCAO, middle cerebral artery occlusion; MCP-1, monocyte chemoattractant protein-1; MMP9, matrix metalloproteinase 9; MRI, magnetic resonance imaging; NeuN, neuronal nuclei; pMCAO, permanent middle cerebral artery occlusion; SDF1α, stromal cell-derived factor 1α; SVZ, subventricular zone; TLR4, toll-like receptor 4; t-PA, tissue plasminogen activator

ISCHEMIC STROKE IS A DEVASTATING illness and the second cause of death and disability worldwide after cardiac ischemia. Currently, thrombolysis with tissue plasminogen activator (t-PA) is the only effective therapy for the acute-phase of stroke, however, owing to the narrow therapeutic window of <4.5 h and safety concerns, fewer than 5% of stroke patients receive this treatment, reaching an effective reperfusion in ~50% of them. In contrast, a broader window exists to promote repair in late phases and to decrease stroke-associated disability. Therefore, stroke remains an enormous therapeutic challenge. Therapies based on immunomodulation, although promising, require a better understanding of the reciprocal interaction between the brain and the immune system.

Innate immunity, promoting inflammatory response, participates in the brain damage produced by ischemia. Indeed, we and others demonstrated the implication of toll-like receptor 4 (TLR4), a receptor with a fundamental role in the activation of the innate immunity, in the acute cerebral damage and in the inflammatory response elicited by an ischemic injury (1–4). In addition, TLR4 appears to play an important role in adult neurogenesis. In this context, Schwartz *et al.* (5) showed the implication of TLR4 in the modulation of the hippocampal neurogenesis in the adult rat under physiological conditions. Both *in vitro* and *in vivo* studies demonstrated that TLR4 induces an inhibition of neuronal proliferation and differentiation. Nevertheless, the role of TLR4 and the mechanisms that regulate neurogenesis in pathological situations such as stroke are still unknown.

Therefore, this study aims to determine the role of TLR4 on neurogenesis in pathological conditions by studying proliferation, migration, and differentiation processes after experimental stroke induced by an occlusion of the middle cerebral artery (MCA) in TLR4-deficient mice (C57BL/10ScNJ) and animals that express TLR4 normally.

[1] These authors contributed equally to this work.

[2] Correspondence: Unidad de Investigación Neurovascular, Departamento de Farmacología, Facultad de Medicina, Universidad Complutense, Avda. Complutense s/n, 28040, Madrid, Spain. E-mail: ignacio.lizasoain@med.ucm.es

doi: 10.1096/fj.14-252452

0892-6638/14/0028-4710 © FASEB

MATERIALS AND METHODS

Animals

Adult male C57BL/10ScNJ and C57BL/10J mice (2–3 mo) were used (Jackson Laboratory, Bar Harbor, ME, USA). The murine strain C57BL/10ScNJ does not express TLR4 because of a naturally total deletion of the TLR4 gene (6). C57BL/10J substrain does not express the mutation, and it is considered as the wild-type group ($TLR4^{+/+}$ group). All experimental protocols adhered to the guidelines of the Animal Welfare Committee of the Universidad Complutense (EU directives 86/609/CEE and 2003/65/CE). Mice were housed under standard conditions of temperature and humidity and a 12-h light-dark cycle (lights on at 08:00) with free access to food and water.

Induction of permanent focal ischemia

All groups were performed and quantified in a randomized fashion (coin toss) by investigators blinded to each specific treatment. Surgery leading to focal cerebral ischemia was conducted under anesthesia with isoflurane in a mix of O_2 and N_2O (0.2/0.8 L/min). During surgery, body temperature was maintained at 37.0 ± 0.5°C using a servo-controlled rectal probe–heating pad. Mice were subjected to a permanent MCA occlusion (pMCAO) described by Chen *et al.* (7). A small craniotomy was made over the trunk of the left MCA and above the rhinal fissure. The pMCAO was done by ligature of the trunk just before its bifurcation between the frontal and parietal branches with a 9–0 suture (proximal occlusion). To obtain smaller infarct volumes and thus to avoid the bias due to different infarct sizes on the end points of the study, we included an additional group in which the occlusion was performed in the same way but more distally, at a posterior branch of the MCA of $TLR4^{+/+}$ mice (distal occlusion). The resulting infarcted areas were similar, and the quantifications were carried out in the central regions, where the differences are not significant. Complete interruption of blood flow was confirmed under an operating microscope. Sham surgery animals, considered as control group, were subjected to anesthesia and to the surgical procedure, but the occlusion of the arteries was omitted.

Physiological parameters (rectal temperature, mean arterial pressure, pO_2, pCO_2, pH) were not significantly different between all studied groups (data not shown). No spontaneous mortality was found after MCAO with this model, and this was unaffected by the different experimental groups. 5-Bromo-2′-deoxyuridine (BrdU, 50 mg/kg) was injected intraperitoneally once daily from d 5 to 6 after ischemia. Cell proliferation was quantified at 7, 14, and 28 d after ischemia by immunohistochemical studies.

Infarct size determination

For infarct size determination 2 d after MCAO, magnetic resonance imaging (MRI) examination was performed using a BioSpec BMT 47/40 (Bruker, Ettlingen, Germany). Infarct volume was calculated using ImageJ 1.44l (U.S. National Institutes of Health, Bethesda, MD, USA) from the T2-weighted images.

In addition, infarct volume was determined by Nissl staining at later times: Animals subjected to pMCAO were killed at 7, 14, and 28 d after surgery and subjected to perfusion fixation with 4% p-formaldehyde in 0.1 M phosphate buffer (pH 7.4); brains were then frozen, serially sectioned at 40 μm, and stained with conventional histological Nissl (0.1% cresyl violet) staining. With the observer masked to the experimental conditions, the areas of the infarcted tissue (A_{Inf}), the whole ipsilesional hemisphere (A_{Ips}), and the whole contralesional hemisphere (A_{Contr}) were delineated for each slice. Then, infarct volume (V_{Inf}), expressed as percentage of the hemisphere that is infarcted ($\%H_{Inf}$), was calculated as described previously (8) using the formula $\%H_{Inf} = V_{Inf}/V_{Contr} * 100$, where $V_{Inf} = \sum A_{Inf\_i}/SI_i$, SI is swelling index, $V_{Contr} = \sum A_{Contr\_i}$, and $SI_i = A_{Ips\_i}/A_{Contr\_i}$.

Immunofluorescence staining

Animals (n=6–7/group) were killed at 7, 14, or 28 d after MCAO by pentobarbital overdose followed by transcardiac perfusion through the left ventricle with 0.1 M phosphate buffer as a vascular rinse, followed by a fixing solution containing 4% p-formaldehyde in 0.1 M phosphate buffer (pH 7.4). Brains were removed, postfixed overnight, and placed in 30% sucrose for 48 h. Coronal series sections (40 μm) were cut on a freezing microtome (Leica SM2000R; Leica Microsystems GmbH, Wetzlar, Germany) and stored in cryoprotective solution. Double-label immunofluorescence was performed on free-floating sections and incubated overnight at 4°C with the primary antibodies rat anti-BrdU (1:100; ABD Serotec, Bio-Rad Laboratories Inc., Hercules CA, USA), mouse anti-TLR4 (1:20; Abcam plc, Cambridge, UK), anti-doublecortin (DCX; 1:500; Santa Cruz Biotechnology, Heidelberg, Germany), anti-neuronal nuclei (NeuN; 1:200; MAB 377; Millipore, Billerica MA, USA), and anti-glutamic acid decarboxylase 67 (GAD67; 1:200; Abcam). After incubating with the primary antibody, sections were washed and incubated with the appropriate fluorescent secondary antibody: goat anti-rabbit biotin and horse anti-goat biotin (Vector Laboratories, Peterborough, UK) in combination with Alexa488 streptavidin (Molecular Probes; Life Techologies, Madrid, Spain), Alexa647 (Invitrogen SA, Barcelona, Spain), and donkey Cy3 anti-rat/anti-mouse (Jackson Immunoresearch, Suffolk, UK). Controls performed in parallel without primary antibodies showed very low levels of nonspecific staining.

Cell and optical density quantification on confocal images

For the study of neuroblasts (DCX^+ cells), immunofluorescence images were obtained in a blinded manner from 4 correlative slices of each brain. Stacks at ×20 of the subventricular zone (SVZ; Z_1) were obtained. In addition, two adjacent images (Z_2 and Z_3) along the corpus callosum were also obtained. With the ImageJ 1.44l software, each image was converted into a binary image, and the integrated density (D_{Int}) was calculated. D_{Int} is a calculus of the mean stained area times the intensity of stain in each pixel in the area and indicates the total amount of staining material in that area.

For neuronal differentiation ($BrdU^+/NeuN^+$ cells), immunofluorescence images were taken from 5 correlated sections beginning at 1.70 mm from bregma (until 0.02 mm). The images were taken at ×40, spaced 400 μm from each other. The entire top of the cortex was traced and 800 μm below the stroke, using as boundaries the corpus callosum and the end of the cortex, by analyzing a total of ~16–18 images per hemisphere and section.

Unbiased stereology

The total volume of the dorsolateral striatal extension of the SVZ was estimated by the application of the Cavalieri principle on 7 serial sections per brain (40 μm thickness, 0.32 mm apart; bregma 1.70 to −0.54 mm). The morphological criteria used for the consistent delineation of the SVZ are described elsewhere (9). Stereological estimation of the total number of

$BrdU^+$ cells in the dorsolateral extension of the SVZ was performed using the optical fractionator method (10). The specific parameters used for stereological sampling and quantification of $BrdU^+$ cells are summarized in **Table 1**.

Brain dissociation and cell suspensions analysis by flow cytometry

Brain cell suspensions were prepared as described previously (11, 12). Briefly, at 1 and 2 d after MCAO, mice brain is rapidly removed. SVZs were dissected with a scalpel, placed into 15 ml of ice-cold PBS and dissociated in a single cell suspension using a gentleMACS Dissociator (Miltenyi Biotec, Madrid, Spain) with mechanical and enzymatic digestion according to the manufacturer's instructions. Cell suspension was filtered on 40 μm nylon mesh strainers and centrifuged at 300 *g* for 10 min at room temperature. Pellets were resuspended on 200 μl of 5% BSA in PBS with Fc block reagent. Cell suspensions were colabeled with antibodies for TLR4/MD2 complex (PE/Cy7 anti-TLR4/MD2 and its PE/Cy7 isotype control; BioLegend, San Diego, CA, USA), neural stem cell marker [anti-prominin1/CD133 (APC); Miltenyi Biotec], a major marker of primitive neural stem cell (PE anti-nestin; R&D Biolegend, London, UK) and a marker for proliferative progenitors [epidermal growth factor receptor (EGFR), FITC anti-EGFR; Invitrogen; Life Technologies). For labeling the cytoplasmic protein nestin, suspensions were mixed with permeabilization solution (BD Cytofix/Cytoperm Kit; BD Biosciences, Madrid, Spain) for 20 min at 4°C. Stained cells from cortex and SVZs were washed and resuspended in 300 μl of FACS Flow (BD Pharmingen, San Jose, CA, USA), and the whole suspension was acquired using a FACSCalibur flow cytometer with CellQuest software (BD Pharmingen). Isotype controls (Miltenyi Biotec) were used in parallel.

Statistical analysis

Data are expressed as means ± SD. Comparisons between groups were performed using unpaired Student's *t* test or 1-way ANOVA with the Student-Newman Keuls *post hoc* test for multiple comparisons. Comparisons of semiquantitative scores were analyzed with nonparametric Mann-Whitney *U* test. Linear association between 2 variables was determined by the Pearson correlation coefficient. Differences were considered significant at $P < 0.05$.

RESULTS

Effect of TLR4 on SVZ cell proliferation

TLR4 has been reported to inhibit cell proliferation under physiological conditions (5). However, we could not find any differences in the number of $BrdU^+$ cells 7 and 14 d after stroke when $TLR4^{+/+}$ and $TLR4^{-/-}$ mice were compared ($TLR4^{+/+}$ *vs.* $TLR4^{-/-}$, $P>0.05$; **Fig. 1*A***).

Notably, and in agreement with our previous data (1), $TLR4^{+/+}$ mice presented significantly higher infarct volumes than TLR4-deficient mice (Fig. 1*B*, $P<0.05$), a finding that might be involved in lack of effect of TLR4 on SVZ cell proliferation. To ascertain this issue, we studied whether infarct size was affecting SVZ cell proliferation after stroke. For that, two groups of normal mice were established: a first group in which MCAO was performed on the trunk of the artery (proximal occlusion) and a second group in which the occlusion was made on the posterior branch of the MCA (distal occlusion). As expected, the group with the distal occlusion had significantly smaller infarct volumes after the ischemic injury than the proximal occlusion group (**Fig. 2*A***; $P<0.05$). Interestingly, those mice exposed to MCA proximal occlusion presented higher numbers of $BrdU^+$ cells at the SVZ at 7d than the group with a distal occlusion (Fig. 2*B*; proximal MCAO *vs.* distal MCAO; $P<0.05$). A strong positive correlation was found between infarct size and cell proliferation ($BrdU^+$ cells) determined at the ipsilateral SVZ 7d after injury (Fig. 2*C*; $r=0.812$, $n=10$, $P<0.05$). Furthermore, this correlation became negative when SVZ proliferation was measured 14 d after the injury ($r=-0.909$, $n=10$, $P<0.05$), a time at which a large proportion of newly proliferated cells may have migrated to other areas.

Therefore, to study the effect of TLR4 on SVZ cell proliferation without the influence of lesion size, a distal occlusion in $TLR4^{+/+}$ and a proximal occlusion in $TLR4^{-/-}$, which induce similar infarct volumes (**Fig. 3*A***; $n=8$, $P>0.05$), were compared for subsequent studies. Our data demonstrate that the presence of TLR4 inhibits SVZ cell proliferation after MCAO, as demonstrated by a decreased number of $BrdU^+$ cells in the ipsilateral SVZ, determined 7 d after the ischemic insult, when compared with the $TLR4^{-/-}$ group with similar infarct size (Fig. 3*B*, $TLR4^{+/+}$ MCAO *vs.* $TLR4^{-/-}$ MCAO, $P<0.05$). Regarding sham surgery $TLR4^{+/+}$ mice, values of $BrdU^+$ cells in the SVZ were higher than those present in the MCAO group (Fig. 3*B*), which suggests an increased migration after MCAO. However, no differences were found between sham-operated and MCAO in the TLR4-deficient group (Fig. 3*B*). Naive values were similar to those of sham-operated animals (data not shown).

TABLE 1. *Parameters used for the stereological quantification of $BrdU^+$ cells in the SVZ*

	7 d			14 d		
Parameter	$TLR4^{+/+}$ proximal	$TLR4^{+/+}$ distal	$TLR4^{-/-}$	$TLR4^{+/+}$ proximal	$TLR4^{+/+}$ distal	$TLR4^{-/-}$
Counting frame area (mm^2)	100 (10×10)			100 (10×10)		
Sampling sites per brain	495 ± 32	494 ± 121	511 ± 69	369 ± 39	364 ± 77	335 ± 48
Total BrdU+ cells	346 ± 41	262 ± 134	313 ± 64	117 ± 35	162 ± 86	136 ± 41
CE, Gundersen, $m = 0$	0.11 ± 0.03	0.13 ± 0.03	0.12 ± 0.02	0.12 ± 0.03	0.12 ± 0.02	0.12 ± 0.02

Coefficient of error (CE) is a method for estimating the precision of the estimate described by Gundersen *et al.* (10). Values are means ± SD.

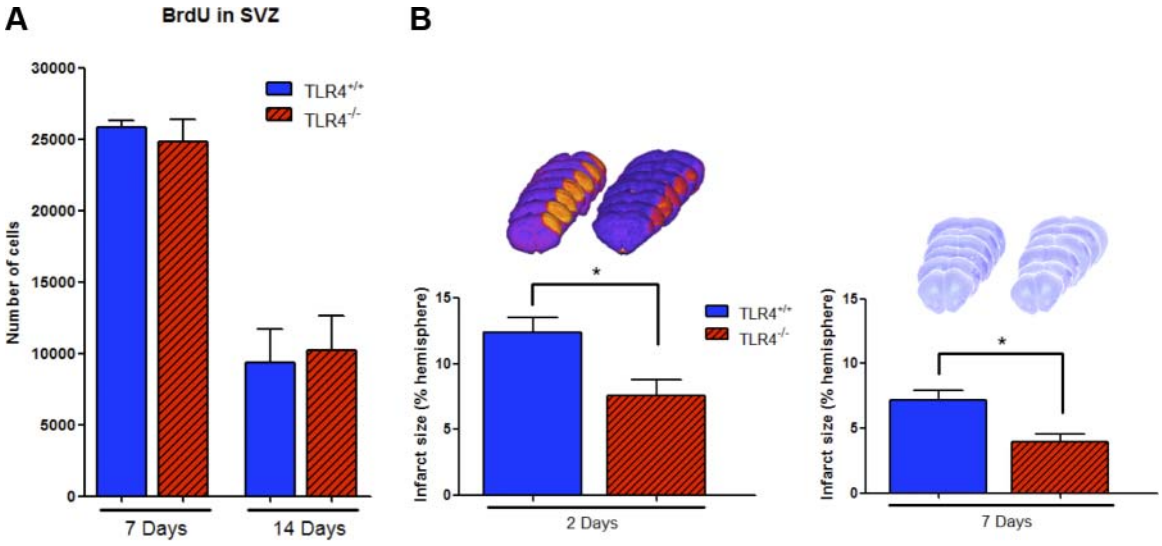

Figure 1. Effect of TLR4 on SVZ proliferation. *A*) Number of BrdU$^+$ cells in the SVZ at 7 and 14 d after MCAO in mice that express TLR4 normally (blue columns; C57BL/10J mice: *TLR4*$^{+/+}$) and in TLR4-deficient mice (red columns; C57BL/10ScNJ mice: *TLR4*$^{-/-}$). *B*) Infarct size was determined by MRI (2 d) and Nissl (7 d) after MCAO in *TLR4*$^{+/+}$ and *TLR4*$^{-/-}$ mice. Data are means ± SD, $n = 6–8$. *$P < 0.05$.

To confirm this finding and to establish the nature of the cells present in the SVZ, we also characterized by flow cytometry the different cell types present in this area at earlier times, 1 and 2 d after MCAO. First, our results show the presence of two major cell populations: a prominin-1$^+$/EGFR$^+$/nestin$^+$ cell subset, corresponding to the primary neural stem cells (astrocyte-like type B cells), and a prominin-1$^+$/EGFR$^+$/nestin$^-$ cell subset, consistent with the transit-amplifying cells (type C cells). Notably, whereas in the prominin-1$^+$/EGFR$^+$/nestin$^+$ population no differences were found between groups (Fig. 3*C*), *TLR4*$^{+/+}$ mice showed a smaller number of prominin-1$^+$/EGFR$^+$/nestin$^-$ cells than the *TLR4*$^{-/-}$ mice after MCAO (Fig. 3*C*; *TLR4*$^{+/+}$ MCAO *vs.* *TLR4*$^{-/-}$ MCAO; $P<0.05$), and also than its own sham surgery condition ($P<0.05$; Fig. 3*C*), which suggests an inhibitory role of TLR4 in the proliferation of type C cells after stroke.

Effect of TLR4 on neuroblasts migration toward the injured area

We next explored the effect of TLR4 on the neuroblast population (type A cells) in 3 migratory zones,

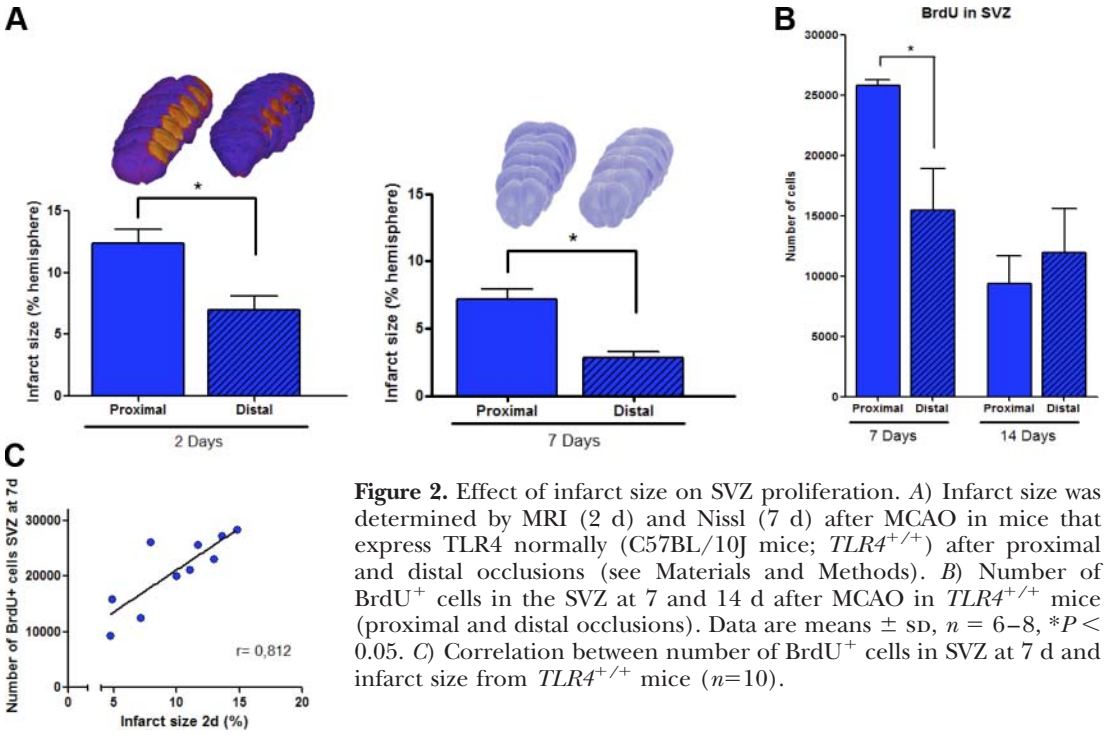

Figure 2. Effect of infarct size on SVZ proliferation. *A*) Infarct size was determined by MRI (2 d) and Nissl (7 d) after MCAO in mice that express TLR4 normally (C57BL/10J mice; *TLR4*$^{+/+}$) after proximal and distal occlusions (see Materials and Methods). *B*) Number of BrdU$^+$ cells in the SVZ at 7 and 14 d after MCAO in *TLR4*$^{+/+}$ mice (proximal and distal occlusions). Data are means ± SD, $n = 6–8$, *$P <$ 0.05. *C*) Correlation between number of BrdU$^+$ cells in SVZ at 7 d and infarct size from *TLR4*$^{+/+}$ mice (n=10).

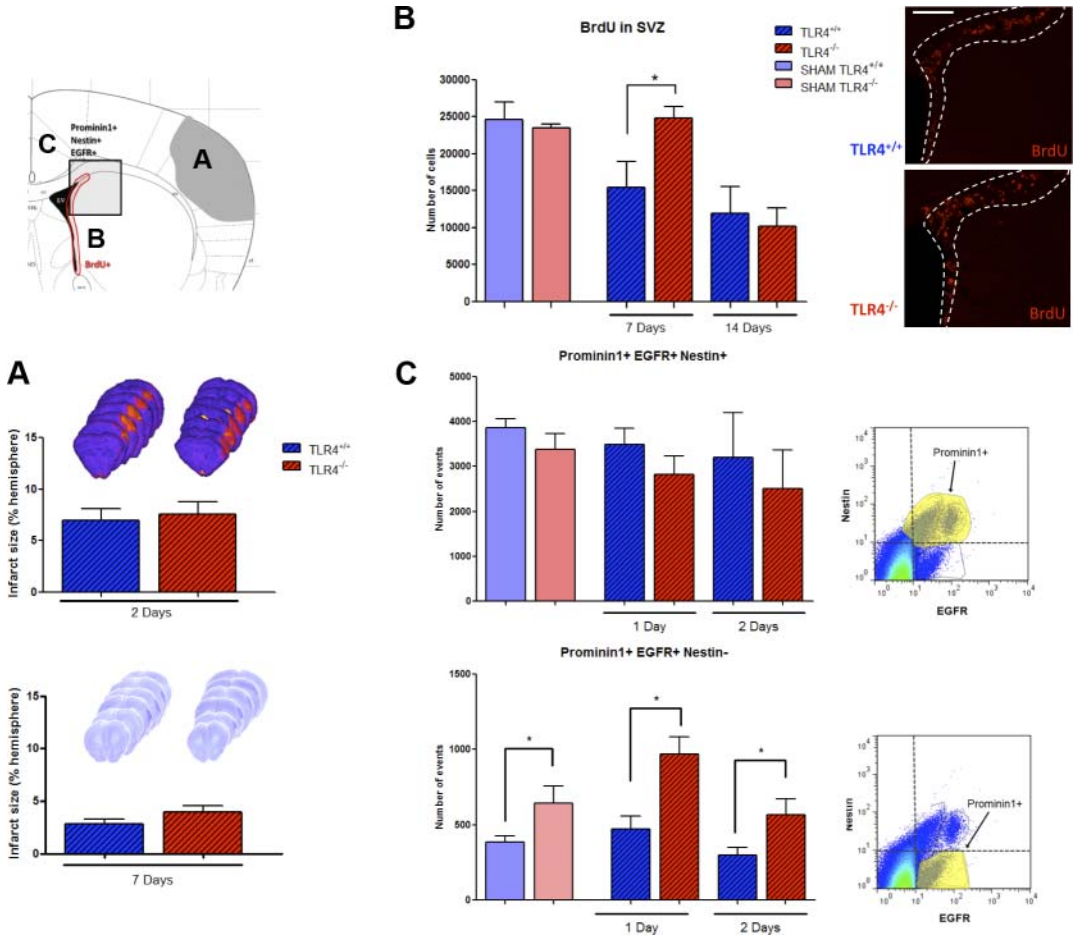

Figure 3. Effect of TLR4 on SVZ proliferation in groups with similar infarct sizes. *A*) Infarct size was determined by MRI (2 d) and Nissl (7 d) after MCAO in mice that express TLR4 normally (blue columns; C57BL/10J mice: $TLR4^{+/+}$, distal occlusion) and in TLR4-deficient mice (red columns; C57BL/10ScNJ mice: $TLR4^{-/-}$, proximal occlusion) (see Materials and Methods). *B*) Number and representative images of $BrdU^+$ cells in the SVZ at 7 and 14 d after sham surgery and MCAO in $TLR4^{+/+}$ and $TLR4^{-/-}$ mice. Scale bar = 200 μm. *C*) Flow cytometric analysis of the SVZ for neural stem cells. Representative dot plots and number of prominin-1^+/$EGFR^+$/$nestin^+$ and prominin-1^+/$EGFR^+$/nestin- cells in the SVZ obtained 1 and 2 d after MCAO from $TLR4^{+/+}$ (blue columns) and $TLR4^{-/-}$ (red columns) mice. Cell suspensions were labeled with antibodies for the different markers and analyzed by flow cytometry (see Materials and Methods). Data are means ± SD, $n = 6–8$. $^*P < 0.05$.

which ranged from the SVZ (Z_1) through the corpus callosum (Z_2) toward the damaged area (Z_3), 7 and 14 d after the ischemic insult. We found that the density of neuroblasts (DCX^+ cells) in Z_3, but not in Z_1 and Z_2, was higher in $TLR4^{+/+}$ when compared with TLR4-deficient mice 7 d after MCAO, consistent with a faster migration process in $TLR4^{+/+}$ animals. Notably, 14 d after MCAO, the density of DCX^+ cells in all the migratory zones studied decreased in $TLR4^{+/+}$ when compared with TLR4-deficient mice (**Fig. 4**; $TLR4^{+/+}$ MCAO *vs.* $TLR4^{-/-}$ MCAO, $P<0.05$). These results suggest that, in $TLR4^{+/+}$ mouse brain, neuroblasts migrate faster toward the injured area, whereas a hampered migration is found in TLR4-deficient animals. In sham surgery mice, neuroblasts density was smaller than that present after MCAO in both groups of mice (**Table 2**). Naive values were similar to those of sham surgery animals. We did not find any significant correlation between SVZ cell proliferation and neuroblast migration (data not shown).

Expression of TLR4 on type A, B, and C cells

We have studied the expression of TLR4 on type A cells by immunofluorescence staining in brain sections. We have found that neuroblasts (DCX^+ cells) do not express TLR4 in the SVZ, 7 d after the ischemic insult (**Fig. 5*A***). In addition, using flow cytometry, we show that most type B cells (prominin-1^+/$EGFR^+$/$nestin^+$ cells) express TLR4 1 d after MCAO, whereas only a 42% of type C cells (Prominin-1^+/$EGFR^+$/$nestin^-$ cells) do (Fig. 5*B*).

Effect of TLR4 on the number of new neurons in the peri-infarct cortex

Finally, we have studied the number of adult differentiated neurons ($BrdU^+$/$NeuN^+$ cells) in the ipsilesional cortex at 14 and 28 d after the ischemic insult. Interestingly, we found that the presence of TLR4 increased the number of $BrdU^+$/$NeuN^+$ cells, at both 14 and 28 d, when compared with the group of $TLR4^{-/-}$

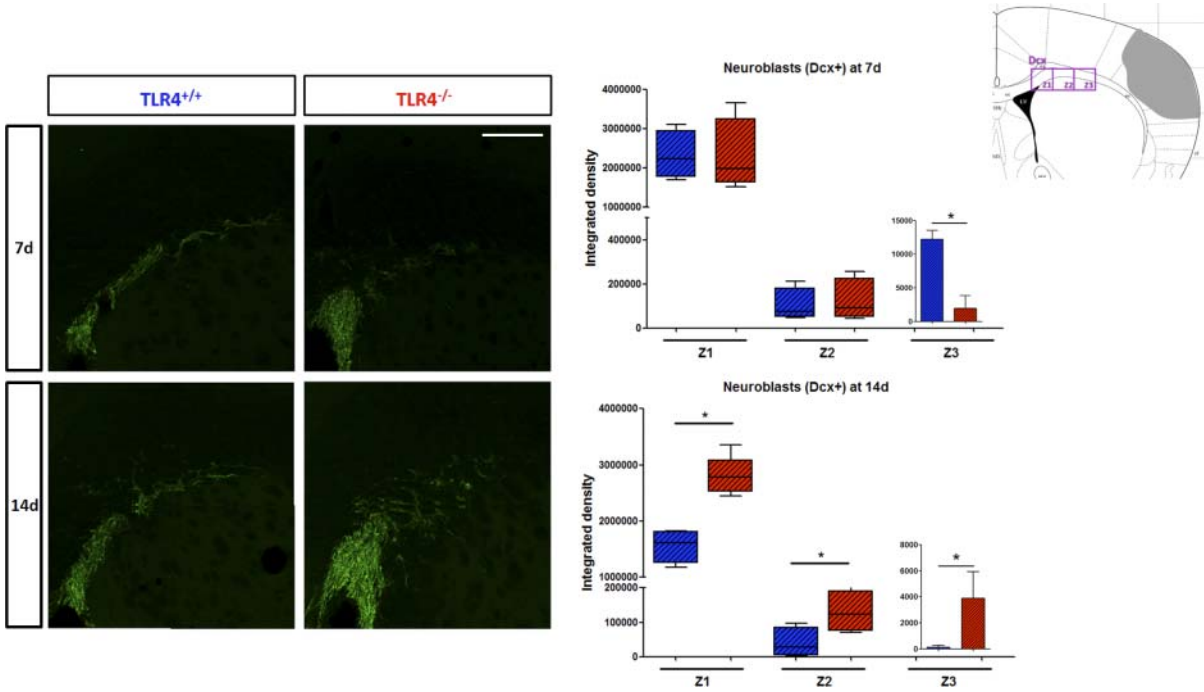

Figure 4. Effect of TLR4 on neuroblast migration. Representative images and number of neuroblasts (DCX^+ cells) in 3 migratory zones (Z_1, Z_2, Z_3) at 7 and 14 d after MCAO in $TLR4^{+/+}$ (blue columns) and $TLR4^{-/-}$ (red columns) mice. Migratory zones were established from the SVZ (Z_1) through the corpus callosum (Z_2) toward the damaged area (Z_3) (see Materials and Methods). Scale bar = 200 μm. Data are means ± SD, $n = 6–8$. *$P < 0.05$.

mice (**Fig. 6*A***; $TLR4^{+/+}$ MCAO *vs.* $TLR4^{-/-}$ MCAO, $P<0.05$). We have also characterized the new neurons by using an interneuron marker (GAD67). Thus, we found that most $BrdU^+/NeuN^+$ cells in the peri-infarct cortex 14 d after ischemic injury were interneurons, as shown by its staining with anti-GAD67 (Fig. 6*B*). These results demonstrate that, despite reduced SVZ cell proliferation, the number of new interneurons in the peri-infarct cortex is increased in $TLR4^{+/+}$ mice. No new neurons ($BrdU^+/NeuN^+$) were found in the cortex of naive/sham surgery mice (data not shown).

DISCUSSION

In this study, we have explored the role of TLR4 on neurogenesis after stroke by using a permanent model of focal ischemia in mice expressing or not expressing TLR4. Our data show that cell proliferation ($BrdU^+$ cells) at the SVZ is dependent on infarct size after stroke; TLR4 inhibits SVZ cell proliferation, as shown by a decreased number of prominin-$1^+/EGFR^+/nestin^-$ cells (transit-amplifying or type C cells) 1 and 2 d and of $BrdU^+$ cells 7 d after stroke; TLR4 promotes the migration of neuroblasts, as shown by the fact that they can reach a farther distance at earlier times after stroke (7 d) in $TLR4^{+/+}$ mice, whereas they accumulate in all the migratory zones studied at late times (14 d) in TLR4-deficient mice, and consistently, $TLR4^{+/+}$ mice present a higher number of mature neurons, which show a GABAergic phenotype ($NeuN^+/BrdU^+/GAD67^+$ cells) consistent with interneurons, in the peri-infarct cortical area at 14 and 28 d after stroke.

To our knowledge, we report for the first time that SVZ cell proliferation, under ischemic conditions, depends on infarct size, as shown by the strong positive

TABLE 2. *Neuroblasts (DCX^+ cells), measured as integrated density, in two migratory zones at 7 and 14 d after sham surgery or MCAO treatment in* $TLR4^{+/+}$ *and* $TLR4^{-/-}$ *mice*

	$TLR4^{+/+}$		$TLR4^{-/-}$	
Time	Sham	MCAO	Sham	MCAO
7 d				
Z_1	1.168.585 ± 273.200	2.511.435 ± 311.601	1.533.636 ± 229.247	2.335.930 ± 486.545
Z_2	9.818 ± 2.098	101.499 ± 37.327	10.277 ± 2.894	121.420 ± 48.250
14 d				
Z_1	929.564 ± 87.329	1.562.017 ± 151.960	887.412 ± 82.941	2.799.765 ± 163.940*
Z_2	39.811 ± 5.093	38.321 ± 4.040	30.346 ± 4.894	130.044 ± 13.322*

See Materials and Methods. *$P < 0.05$ vs MCAO $TLR4^{+/+}$.

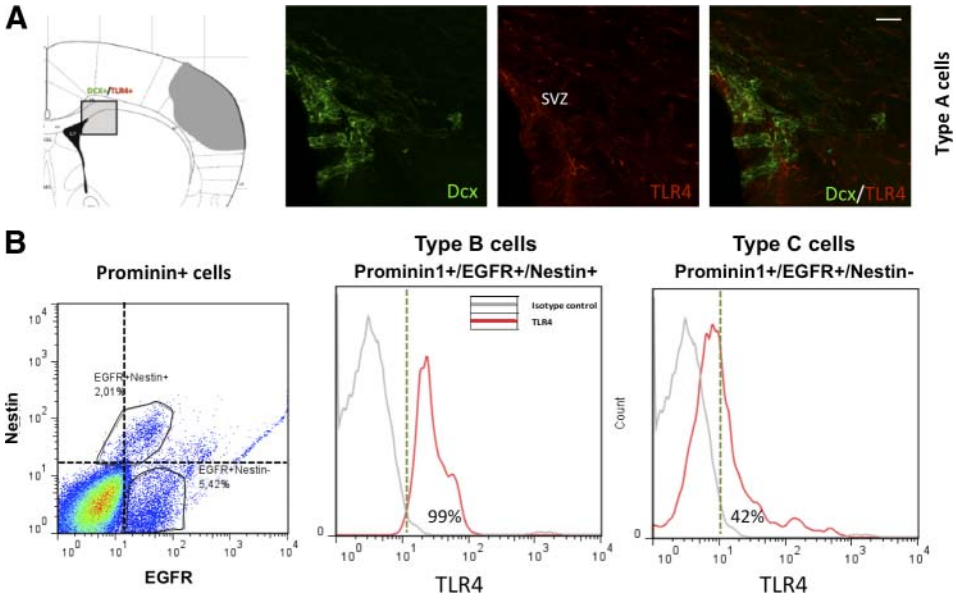

Figure 5. Expression of TLR4 on type A, B, and C cells. *A*) Double immunofluorescence of neuroblasts (DCX; green) in combination with TLR4 (red) in the SVZ at 7 d after MCAO in *TLR4*$^{+/+}$ mice. Scale bar = 50 μm. *B*) Flow cytometric analysis of the SVZ for TLR4 expression. Representative dot plot and percentage of prominin-1^{+}/EGFR^{+}/nestin^{+} and prominin-1^{+}/EGFR^{+}/nestin^{-} cells, which express TLR4 in the SVZ, obtained 1 d after MCAO.

correlation found between infarct size and cell proliferation determined at the ipsilateral SVZ 7 d after the injury. It has been reported that large striatal ischemic lesions are accompanied by an increased proliferation at the SVZ in rats (13–15); however, the effect of cortical lesions in mice and its direct relationship with the size of the damaged area had not been described. Interestingly, the correlation was negative when determined 14 d after the lesion. This finding can be explained by the BrdU labeling protocol used, which underestimates the proliferating population in the SVZ after stroke, due to the fact that labeled cells are only those proliferating when the BrdU pulse is applied, corresponding to d 5–6 after MCAO and, more important, that stroke not only affects SVZ cell proliferation but also enhances the migration process of the new cells toward the site of damage (15–18), decreasing the number of proliferating cells at the SVZ and resulting in no apparent changes when compared between different time points. Therefore, the number of proliferating cells at a certain time point in the SVZ results from the balance between proliferation and migration.

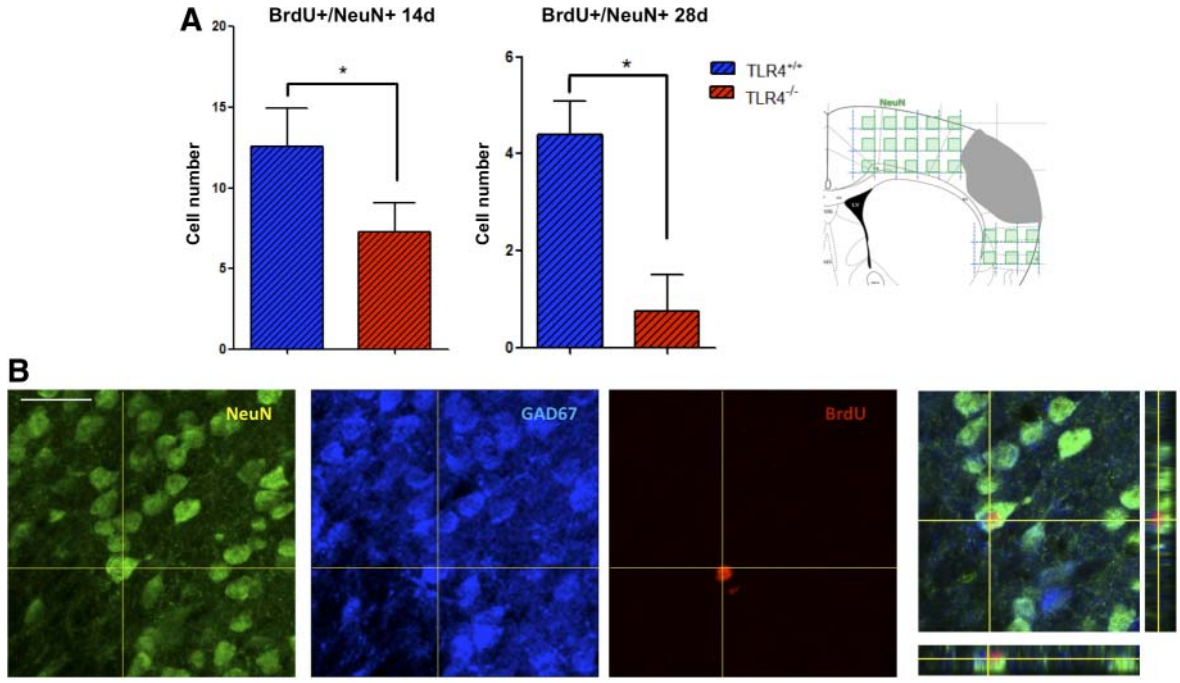

Figure 6. Effect of TLR4 on the number of new neurons in the peri-infarct cortex. *A*) Number of adult differentiated neurons (BrdU^{+}/NeuN^{+} cells) in the ipsilesional cortex at 14 and 28 d after MCAO in *TLR4*$^{+/+}$ (blue columns) and *TLR4*$^{-/-}$ (red columns) mice. Data are means ± SD, n = 6–8. *$P < 0.05$. *B*) Representative immunofluorescence staining of brain sections. Orthogonal projection of NeuN (green) and BrdU (red) in combination with GAD67 (blue) in *TLR4*$^{+/+}$ mice at 14 after MCAO. Scale bar = 25 μm.

In this context, our data obtained in sham surgery animals showing higher values to those present in the ischemic group, despite the positive correlation with lesion size at 7 d, also support this affirmation and are consistent with the proliferating population (15–21%) described in postnatal animals (19, 20). However, no correlation was found between SVZ cell proliferation and neuroblast migration, suggesting that the number of $BrdU^+$ cells at the SVZ at the times studied is not only affected by migration but also by modulation of proliferation.

Second, and in line with our previous suggestion, our data show that the presence of TLR4 inhibits SVZ cell proliferation, as demonstrated by a decreased number of prominin-1^+/$EGFR^+$/$nestin^-$ cells at 1 and 2 d (flow cytometry analysis), and of $BrdU^+$ cells at 7 d after the ischemic insult in the ipsilateral SVZ when compared with the group of *TLR4*$^{-/-}$ mice with a similar infarct size. Specifically, our results show that the presence of TLR4 inhibits the proliferation of the population of prominin-1^+/$EGFR^+$/$nestin^-$ cells, which likely correspond to transit-amplifying cells (type C cells), as described for the subgranular zone (transit-amplifying type 3 cells; ref. 21) and which are cells in a stage prior to becoming neuroblasts (type A cells) but still maintaining their proliferative potential ($EGFR^+$). In contrast, astrocyte-like type B cells and proliferative type C cells (2a and 2b; prominin-1^+/$EGFR^+$/$nestin^+$) do not seem to be affected by TLR4. Thus, our present data are the first demonstration of the inhibitory role of TLR4 on SVZ neural cell proliferation after an ischemic insult. In agreement with our data, it has been shown that TLR4 inhibits proliferation in the SVZ (5) in physiological conditions, but the cell type involved or the effect under pathological conditions remained unexplored. Of note, we have found that type B and 42% of type C but not type A cells express TLR4. This is in apparent controversy with our functional findings, since the population with a majority expression of TLR4 (type B cells) was not affected by the lack of this receptor, whereas the cell subset with a heterogeneous TLR4 expression was. A possible explanation is that TLR4 affects cell proliferation only in some cell subsets, as is the case with the proliferative subset of type C cells that we have described. In addition, the effect of TLR4 on cell proliferation might be indirect, in such a way that other cells, such as "surveillant" microglial cells in charge of the elimination of newborn cells by phagocytosis (22), could be the direct effectors of TLR4 activation by regulating cell number of a "departing" target type B population. Further studies are required to elucidate this issue.

Third, we have shown that deficiency of TLR4 delays the neuroblast migration process from the SVZ toward the damaged area. In our study, we examined the neuroblast population (type A cells; DCX^+) in 3 migratory zones ranging from the SVZ (Z_1) through the corpus callosum (Z_2) toward the damaged area (Z_3), at two different times, 7 and 14 d after the ischemic insult. One week after the infarct, more neuroblasts in *TLR4*$^{+/+}$ mice could migrate a farther distance and to reach areas closer to the injured region (Z_3) than those present in sections from TLR4-deficient mice. In contrast, at 14 d, whereas neuroblasts density in the three areas decreased in *TLR4*$^{+/+}$ mice when compared with data from 7 d, consistent with their migration toward the injured area, densities in Z_1–Z_3 of TLR4-deficient mice were similar to values at 7 d, strongly suggesting that TLR4 is crucial for neuroblast migration to damaged areas. A very interesting observation is that MCAO clearly increases neuroblast migration when compared with the respective sham surgery groups, as opposed to the apparent lack of effect or even decrease in proliferation that, as discussed above, is likely due to migration. This finding strongly suggests that the major effect of stroke on the neurogenesis process is exerted at the level of migration, likely driven by intrinsic cues induced by the ischemic injury.

In line with the previous issue and as commented above, stroke can promote the migration of neuroblasts toward the site of damage (15–18), but the mechanisms involved remain to be fully understood. Our studies are the first to indicate that TLR4 is involved in this process. Several studies have demonstrated that up-regulation of monocyte chemoattractant protein-1 (MCP-1) and stromal cell-derived factor 1α (SDF1α) in damaged brain provides the chemokine signals that attract neuroblasts (23–25). In this context, previous data demonstrating that MCP-1 expression is lower in TLR4-deficient mice (26–28) might explain—at least in part—the defective migration in TLR4 deficiency. Furthermore, matrix metalloproteinase 9 (MMP9) is also required for neuroblast migration, as inhibition of matrix metalloproteinases has been demonstrated to significantly suppress the movement of neuroblasts from the SVZ to the damaged tissue (29). Our previous results showing a lower expression of MMP9 in TLR4-deficient mice after stroke (1) might also explain the impaired migration process that we have now described.

Finally, we have found the presence of new neurons ($NeuN^+$/$BrdU^+$ cells) with a GABAergic, interneuron ($GAD67^+$ cells) phenotype in the cortical area at 14 and 28 d after stroke. Notably, TLR4-deficient mice have a lesser number of new neurons, in accordance with the suppression of the migratory process found. Although the number found appears relatively low, it is likely to be remarkably underestimated, as the figures reported only represent the fraction of cells that reach the infarct and differentiate into neurons among those that proliferated at d 5–6 after the injury, when the BrdU pulse was applied.

CONCLUSIONS

Our present data indicate that, despite a negative effect on SVZ cell proliferation, TLR4 plays an important role in stroke-induced neurogenesis by promoting neuroblast migration and increasing the number of new cortical interneurons in the chronic phase of stroke. An interesting possibility is that, in a concerted action, TLR4 curbs a likely excessive neural cell proliferation while at the same time promotes an organized neuroblast migration toward the peri-infarct for an efficient replacement of dead cells in the damaged area after stroke.

To our knowledge, this is the first report demonstrating that TLR4 regulates neurogenesis not only under physiological conditions but also in a pathological setting such as stroke. Despite the evidence showing a deleterious role of TLR4 in the initiation of inflammation and subsequent brain damage in the acute-phase, our present results unravel a new function in this setting, which may be necessary for brain repair, by promoting migration and neurogenesis during the chronic phase of stroke. FJ

The authors thank Tamara Atanes and Roberto Cañadas for technical assistance. This work was supported by the Spanish Ministry of Economy and Innovation, grants SAF2011-23354 (I.L.), SAF2012-33216 (M.A.M.), and CSD2010-00045 (M.A.M.); by the Spanish Ministry of Health and Fondo Europeo de Desarrollo Regional (FEDER), RETICS RD12/0014/0003 (I.L.); and by the Regional Madrid Government, grants S2010/BMD-2336 (M.A.M.) and S2010/BMD-2349 (I.L.). The authors declare no conflicts of interest.

REFERENCES

1. Caso, J. R., Pradillo, J. M., Hurtado, O., Lorenzo, P., Moro, M. A., and Lizasoain, I. (2007) Toll-like receptor 4 is involved in brain damage and inflammation after experimental stroke. *Circulation* **115,** 1599–1608
2. Caso, J. R., Pradillo, J. M., Hurtado, O., Leza, J. C., Moro, M. A., and Lizasoain, I. (2008) Toll-like receptor 4 is involved in subacute stress-induced neuroinflammation and in the worsening of experimental stroke. *Stroke* **39,** 1314–1320
3. Cao, C. X., Yang, Q. W., Lv, F. L., Cui, J., Fu, H. B., and Wang, J. Z. (2007) Reduced cerebral ischemia-reperfusion injury in Toll-like receptor 4 deficient mice. *Biochem. Biophys. Res. Commun.* **353,** 509–514
4. Tang, S. C., Arumugam, T. V., Xu, X., Cheng, A., Mughal, M. R., Jo, D. G., Lathia, J. D., Siler, D. A., Chigurupati, S., Ouyang, X., Magnus, T., Camandola, S., and Mattson, M. P. (2007) Pivotal role for neuronal Toll-like receptors in ischemic brain injury and functional deficits. *Proc. Natl. Acad. Sci. U. S. A.* **104,** 13798–13803
5. Rolls, A., Shechter, R., London, A., Ziv, Y., Ronen, A., Levy, R., and Schwartz, M. (2007) Toll-like receptors modulate adult hippocampal neurogenesis. *Nat. Cell Biol.* **9,** 1081–1088
6. Poltorak, A., He, X., Smirnova, I., Liu, M. Y., Van Huffel, C., Du, X., Birdwell, D., Alejos, E., Silva, M., Galanos, C., Freudenberg, M., Ricciardi-Castagnoli, P., Layton, B., and Beutler, B. (1998) Defective LPS signaling in C3H/HeJ and C57BL/10ScCr mice: mutations in Tlr4 gene. *Science* **282,** 2085–2088
7. Chen, S. T., Hsu, C. Y., Hogan, E. L., Maricq, H., and Balentine, J. D. (1986) A model of focal ischemic stroke in the rat: reproducible extensive cortical infarction. *Stroke* **17,** 738–743
8. Hernandez-Jimenez, M., Hurtado, O., Cuartero, M. I., Ballesteros, I., Moraga, A., Pradillo, J. M., McBurney, M. W., Lizasoain, I., and Moro, M. A. (2013) Silent information regulator 1 protects the brain against cerebral ischemic damage. *Stroke* **44,** 2333–2337
9. Gonzalez, F. F., McQuillen, P., Mu, D., Chang, Y., Wendland, M., Vexler, Z., and Ferriero, D. M. (2007) Erythropoietin enhances long-term neuroprotection and neurogenesis in neonatal stroke. *Dev. Neurosci.* **29,** 321–330
10. Gundersen, H. J., Bagger, P., Bendtsen, T. F., Evans, S. M., Korbo, L., Marcussen, N., Moller, A., Nielsen, K., Nyengaard, J. R., Pakkenberg, B., Sørensen, F. B., Vesterby, A., and West, M. J. (1988) The new stereological tools: disector, fractionator, nucleator and point sampled intercepts and their use in pathological research and diagnosis. *APMIS* **96,** 857–881
11. Campanella, M., Sciorati, C., Tarozzo, G., and Beltramo, M. (2002) Flow cytometric analysis of inflammatory cells in ischemic rat brain. *Stroke* **33,** 586–592
12. LaFrance-Corey, R. G., and Howe, C. L. (2011) Isolation of brain-infiltrating leukocytes. *J. Vis. Exp.* **2011,** 2747
13. Jin, K., Minami, M., Lan, J. Q., Mao, X. O., Batteur, S., Simon, R. P., and Greenberg, D. A. (2001) Neurogenesis in dentate subgranular zone and rostral subventricular zone after focal cerebral ischemia in the rat. *Proc. Natl. Acad. Sci. U. S. A.* **98,** 4710–4715
14. Zhang, R. L., Zhang, Z. G., Zhang, L., and Chopp, M. (2001) Proliferation and differentiation of progenitor cells in the cortex and the subventricular zone in the adult rat after focal cerebral ischemia. *Neuroscience* **105,** 33–41
15. Arvidsson, A., Collin, T., Kirik, D., Kokaia, Z., and Lindvall, O. (2002) Neuronal replacement from endogenous precursors in the adult brain after stroke. *Nat. Med.* **8,** 963–970
16. Luskin, M. B. (1993) Restricted proliferation and migration of postnatally generated neurons derived from the forebrain subventricular zone. *Neuron* **11,** 173–189
17. Zhang, R. L., Zhang, Z. G., Lu, M., Wang, Y., Yang, J. J., and Chopp, M. (2006) Reduction of the cell cycle length by decreasing G1 phase and cell cycle reentry expand neuronal progenitor cells in the subventricular zone of adult rat after stroke. *J. Cereb. Blood Flow Metab.* **26,** 857–863
18. Zhang, R. L., LeTourneau, Y., Gregg, S. R., Wang, Y., Toh, Y., Robin, A. M., Zhang, Z. G., and Chopp, M. (2007) Neuroblast division during migration toward the ischemic striatum: a study of dynamic migratory and proliferative characteristics of neuroblasts from the subventricular zone. *J. Neurosci.* **27,** 3157–3162
19. Schultze, B., and Korr, H. (1981) Cell kinetic studies of different cell types in the developing and adult brain of the rat and the mouse: a review. *Cell Tissue Kinet.* **14,** 309–325
20. Smith, C. M., and Luskin, M. B. (1998) Cell cycle length of olfactory bulb neuronal progenitors in the rostral migratory stream. *Dev. Dynam.* **213,** 220–227
21. Kempermann, G., Jessberger, S., Steiner, B., and Kronenberg, G. (2004) Milestones of neuronal development in the adult hippocampus. *Trends Neurosci.* **27,** 447–452
22. Sierra, A., Abiega, O., Shahraz, A., and Neumann, H. (2013) Janus-faced microglia: beneficial and detrimental consequences of microglial phagocytosis. *Front. Cell. Neurosci.* **7,** 6
23. Imitola, J., Raddassi, K., Park, K. I., Mueller, F. J., Nieto, M., Teng, Y. D., Frenkel, D., Li, J., Sidman, R. L., Walsh, C. A., Snyder, E. Y., and Khoury, S. J. (2004) Directed migration of neural stem cells to sites of CNS injury by the stromal cell-derived factor 1alpha/CXC chemokine receptor 4 pathway. *Proc. Natl. Acad. Sci. U. S. A.* **101,** 18117–18122
24. Robin, A. M., Zhang, Z. G., Wang, L., Zhang, R. L., Katakowski, M., Zhang, L., Wang, Y., Zhang, C., and Chopp, M. (2006) Stromal cell-derived factor 1alpha mediates neural progenitor cell motility after focal cerebral ischemia. *J. Cereb. Blood Flow Metab.* **26,** 125–134
25. Yan, Y. P., Sailor, K. A., Lang, B. T., Park, S. W., Vemuganti, R., and Dempsey, R. J. (2007) Monocyte chemoattractant protein-1 plays a critical role in neuroblast migration after focal cerebral ischemia. *J. Cereb. Blood Flow Metab.* **27,** 1213–1224
26. Chong, A. J., Shimamoto, A., Hampton, C. R., Takayama, H., Spring, D. J., Rothnie, C. L., Yada, M., Pohlman, T. H., and Verrier, E. D. (2004) Toll-like receptor 4 mediates ischemia/reperfusion injury of the heart. *J. Thor. Cardiovasc. Surg.* **128,** 170–179
27. Ao, L., Zou, N., Cleveland, J. C., Jr., Fullerton, D. A., and Meng, X. (2009) Myocardial TLR4 is a determinant of neutrophil infiltration after global myocardial ischemia: mediating KC and MCP-1 expression induced by extracellular HSC70. *Am. J. Physiol. Heart Circ. Physiol.* **297,** H21–H28
28. Dvoriantchikova, G., Barakat, D. J., Hernandez, E., Shestopalov, V. I., and Ivanov, D. (2010) Toll-like receptor 4 contributes to retinal ischemia/reperfusion injury. *Mol. Vis.* **16,** 1907–1912
29. Lee, S. R., Kim, H. Y., Rogowska, J., Zhao, B. Q., Bhide, P., Parent, J. M., and Lo, E. H. (2006) Involvement of matrix metalloproteinase in neuroblast cell migration from the subventricular zone after stroke. *J. Neurosci.* **26,** 3491–3495

Received for publication February 27, 2014.
Accepted for publication July 14, 2014.